Kinetics and Catalysis, Vol. 41, No. 1, 2000, pp. 108–115. Translated from Kinetika i Kataliz, Vol. 41, No. 1, 2000, pp. 122–130.

Mechanism of the Formation of Porous Silicate Mesophases

V. N. Romannikov, V. B. Fenelonov, A. V. Nosov, A. Yu. Derevyankin, S. V. Tsybulya, and V. N. Kolomiichuk

Boreskov Institute of Catalysis, Siberian Division, Russian Academy of Sciences, Novosibirsk, 630090 Russia

Received February 25, 1998

Abstract—The formation of mesoporous mesophase systems prepared by precipitation of soluble forms of SiO_2 at the surface of micelles of cetyltrimethylammonium cations was examined. A molecular mechanism of the formation of a silicate coating and a macroscopic mechanism of the formation of a mesophase were found and discussed. A combination of these mechanisms describes the processes proceeding during the synthesis. It can also explain the observed changes in the structure and texture characteristics of the mesophase.

INTRODUCTION

The development of a crucial new area of the nanotechnology of inorganic materials originated in the 1990s. This innovation is based on the coprecipitation of an inorganic material with a surfactant (S), which is accompanied by self-assembling of liquid-crystal mesophases. Porous materials are formed after the removal of the surfactant from these systems. The texture of these materials corresponds to regular (for example, hexagonal) packing of cylindrical pores with the controlled size in the nanometer range with a corresponding long-range order in the absence of a short-range order [1–5]. Even now these materials, subsequently referred to as MMS (mesoporous mesophase systems or mesoporous molecular sieves), are of considerable interest as acid–base and redox catalysts [1, 3, 4]. In this connection, mechanisms of the formation of these materials are being studied intensively.

Presently, several feasible approaches to the formation of MMS by the interaction of low-molecular-weight inorganic complexes (I) with surfactant molecules (S) are considered in the literature [6–23]. One of these approaches is based on the nonspecific van der Waals interaction between neutral molecules (S^0I^0) [6] or the intermediate formation of a covalent bond between the species (S^0–I^0) [7–11].

The most effective interaction is achieved in systems with the participation of nonionic surfactants and ionic forms of inorganic materials by the Coulomb forces between the oppositely charged S and I ions. In this connection, the development of the concept of reaction mechanisms of the S^+I^- and S^-I^+ types (i.e., the simplest ionic mechanisms) seems to be most topical. It is the S^+I^- mechanism that is responsible for the formation of the most widely studied silicate MMS, which are stable at temperatures up to 700°C [12–23]. This mechanism can be described in general terms using the concept of a stepwise mechanism of the formation of SiO_2-based MMS, which was formulated in the literature and discussed recently in reviews [1–3].

The first step is the interaction of anionic silicate species with the positively charged surface of cationic surfactant micelles in an aqueous solution resulting in the formation of silylated micelles.

At the second step, the self-organization of electrically neutral silylated micelles occurs with the formation of a mesophase. This process proceeds at near-room temperature. However, the primary mesophase formed does not exhibit a reasonably perfect structure, because the self-organization process does not proceed to completion under these conditions.

At the third step, which is usually performed at elevated temperatures (70°C or higher) for a reasonably long time, not only the self-organization of the mesophase is completed, but also the polycondensation of silicate anions proceeds to provide the thermal stability of the structure in general.

However, this concept (in general terms) is quite inadequate to be the basis for optimization of the preparation procedures for catalytically important MMS of not only silicate but also nonsilicate chemical composition. Attempts to describe the mechanism in detail based on published data resulted in contradictions, and answers to some questions are not available in the literature.

In particular, it remains unclear which type of silicate anions of those existing in the initial silicate solution primarily reacts with the charged micellar surface at the first step (multiply charged cubic octamers [18], singly charged dimers [1], or all types of anions but with different probabilities [14]). It is also not quite understood which type of cation–anion interaction (polydentate or monodentate) is preferable in this system.

0023-1584/00/4101-0108$25.00

There is also no clear-cut concept of the structure of the primary mesophase formed at the second step: whether it is a layered material which is then transformed into a hexagonally packed structure [14] or the material is immediately formed as a hexagonal mesophase [17]. Moreover, it is unclear whether the structure of the primary mesophase is retained after the removal of the surfactant by oxidative heat treatment, as in [17], or the material is thermally unstable [1].

The stoichiometry of the reaction of surfactant cations (NR_4^+) with silicate anions is also disputable: what is an estimate of this value and what factors determine this stoichiometry? Why does the formation of a hexagonal silicate mesophase occur even at very low molar concentrations of surfactants in the reaction mixture (however, at concentrations above critical micelle concentrations), in particular, at the molar ratios (NR_4/SiO_2) ≤ 0.2 [17, 21].

In this work, based on a simultaneous analysis of the structure and texture characteristics of MMS with the hexagonal type of packing, we attempted to answer most of these questions and to consider systematically the concepts of the formation of these systems via an ionic reaction mechanism. Silicon dioxide–based MMS (SiO_2–MMS) of the simplest chemical composition were chosen as model test materials.

EXPERIMENTAL

Preparation of initial samples. The syntheses of SiO_2–MMS were performed by hydrothermal treatment of a reaction mixture [12–14, 24, 25] in a batch mode at the molar ratio between components corresponding to the formula

$$SiO_2 \cdot 0.3\ C_{16}H_{33}N(CH_3)_3Br \cdot 0.3\ NaOH \cdot 102\ H_2O.$$

The treatment temperature was 120 ± 5°C; the treatment time (t) varied from 0 to 404 h. The state of SiO_2–MMS immediately after the preparation and homogenization of the starting mixture at room temperature corresponded to zero time. Sodium silicate was used as a source of SiO_2. The pH values in both the starting mixture and final mixtures (i.e., after hydrothermal treatments of different duration) retained within the limits 10.5–11.5. The thermal treatment was performed after filtration, thorough washing with warm water, and drying in air at 40–60°C.

Thermal treatment of initial samples. The thermal treatment was performed in two steps. At the first step, a weighed portion of the air-dry sample was dried to a constant weight at 120 ± 5°C (as a rule, 1.5–2 h was sufficient). We found in special experiments that the dried sample completely regained its initial weight after cooling in air at room temperature for 6 to 7 h. This fact allowed us to conclude that the sample after drying at 120 ± 5°C contains only the cetyltrimethylammonium (Cn) cations $C_{16}H_{33}N(CH_3)_3^+$ and silicate anions (except for terminal SiOH groups). The residual Na_2O concentration in the samples did not exceed 0.05 wt %. At the second step, the dried sample was also calcined to a constant weight in an air flow at 550–580°C (this was usually attained within 3 to 4 h) and then cooled in a dry atmosphere. Considering that the chemical composition of the freshly prepared sample strictly corresponds to the formula SiO_2 (also except for residual terminal SiOH groups), we calculated the composition of the initial form as the molar ratio $C_{16}H_{33}N(CH_3)_3/SiO_2 = NR_4/SiO_2$ from the change in the weight upon the calcination of a dry sample.

Recording of X-ray diffraction patterns. Scanning X-ray patterns of both initial and calcined samples in the air-dry state were recorded on a URD-63 diffractometer using monochromatic CuK_α radiation ($\lambda = 1.54178$ Å) in the 2θ range from 1 to 40° (the scanning rate was 0.5 deg/min). The scanning was also performed in the 2θ range from 1 to 7° at a step of 0.02° and an integration time of 20 s at each point. The characteristic linear dimension of the coherent scattering region (D) was evaluated by the Selyakov–Scherrer equation $D = \lambda[(B - b)\cos\theta]^{-1}$, where B is the half width of the diffraction peak [100], and b is the instrumental broadening.

In order to refine the position of the d_{hkl} reflections and to calculate the unit cell parameter a_0, diffraction patterns were taken in an HPM-1 small-angle X-ray camera. These measurements were performed under conditions of pumping with a fore vacuum pump using CoK_α radiation ($\lambda = 1.7903$ Å) in the 2θ range from 7' (0.117° to 7° at a step of 1' (0.0167°).

Measurement of the true density of samples. The density of calcined SiO_2–MMS samples freshly dried at 120°C for 1.5–2 h was measured with an Autopycnometer-1320 instrument using helium. The density of samples from the examined series was 2.13 ± 0.05 g/cm^3.

Adsorption properties. Calcined samples were examined with an ASAP-2400 Micromeritics setup using nitrogen adsorption at ~77 K according to a standard procedure after evacuation to a residual pressure lower than 10^{-3} torr at 350°C for 12–16 h. A standard isotherm described in [26] was used for plotting comparative graphs.

Calculation of the texture parameters of mesophases. The calculation was performed on the basis of the nitrogen adsorption isotherms according to the procedure described previously [27]. The unit cell parameter of an ideal hexagonal packing of cylinders (a_0) was represented as the sum of the mesopore diameter and the wall thickness of the mesophase:

$$a_0 = d_e + h_w. \quad (1)$$

The a_0 value was determined by X-ray diffraction analysis. For the hexagonal packing, it is expressed by the following well-known relations:

$$a_0 = \frac{2}{\sqrt{3}}d_{100} = 2d_{110} = \frac{4}{\sqrt{3}}d_{200} = 2\frac{\sqrt{7}}{\sqrt{3}}d_{210} = \text{etc.} \quad (2)$$

The mesopore diameter d_M (which is equal to d_ε) can be determined from the volume porosity ε_M by the equation

$$d_M = d_\varepsilon = a_0\left(\frac{2\sqrt{3}}{\pi}\varepsilon_M\right)^{1/2}, \quad (3)$$

where

$$\varepsilon_M = \frac{V_M\rho}{V_M\rho + 1}. \quad (4)$$

That is, this diameter is determined by the mesopore volume V_M and the true density ρ of the mesoporous material, which, like a_0, is the experimentally measured value. In particular, V_M is directly calculated from the comparative graph with a high accuracy. Because the V_M and ρ values enter equation (4) practically as a ratio, even considerable errors in the experimental determination of these values affect an estimate of the mesopore diameter only slightly. Substitution of equations (3) and (4) into (1) results in the expression

$$h_w = a_0\left(1 - \sqrt{\frac{2\sqrt{3}}{\pi}\frac{V_M\rho}{V_M\rho + 1}}\right), \quad (5)$$

which makes it possible to calculate the wall thickness h_w to a high accuracy from direct experimental measurements. Moreover, the use of a comparative procedure provides an opportunity to determine separately the internal surface area of mesopores A_M and the external surface area of mesophase particles A_{ext}.

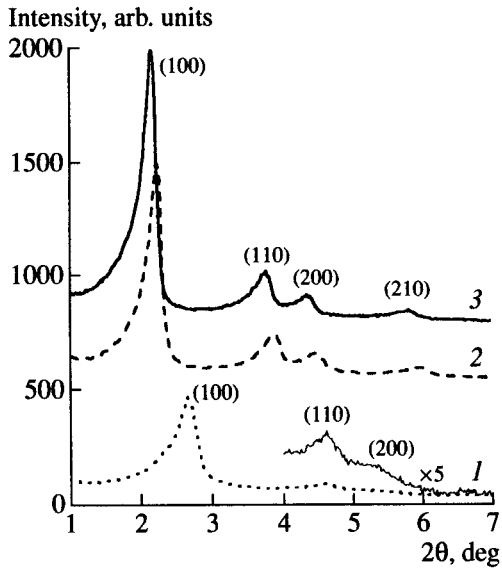

Fig. 1. X-ray diffraction patterns of calcined SiO_2–MMS samples of the C16 series. The duration of hydrothermal treatment, h: (*1*) 0, (2) 20, and (*3*) 404.

RESULTS

The general view of X-ray diffraction patterns of both initial and calcined SiO_2–MMS samples are very similar to the published X-ray diffraction patterns of analogous systems (for example, [24]): they exhibit three reflections at $t = 0$, and four well-resolved reflections in the region of very small angles (2θ from 1° to 7°) at $t \geq 3$ h. In an approximation of ideal hexagonal close packing, these reflections were indicated as (100), (110), (200), and (210). No other reflections in the 2θ region up to 40° were observed. Figure 1 demonstrates typical X-ray diffraction patterns of calcined SiO_2–MMS samples subjected to hydrothermal treatment of different duration.

Table 1 summarizes the results of calculations of structural characteristics of all the examined systems in both initial and calcined forms. It can be seen that going from sample C16-0 to sample C16-3 (i.e., an increase in the phase formation temperature from 20 to 120°C and in the duration of hydrothermal treatment from 0 to 3 h) is accompanied by a significant increase in the unit cell parameter a_0 in both initial and calcined forms. A further increase in the treatment time ($t \geq 3$ h at 120°C) caused no changes in the a_0 parameter in both initial and corresponding calcined forms.

In addition, it can be seen in Table 1 that the reflection (100) was significantly narrowed (the $B[d_{100}]$ value decreased) with increasing t (especially during the initial period of $t \leq 20$ h).

The described changes in X-ray diffraction characteristics occurred with the monotonically decreasing molar fraction of the surfactant cations NR_4^+ in the composition of initial samples (Table 1). In this case, a pronounced decrease in the NR_4/SiO_2 ratio was observed on going from sample C16-0 to sample C16-3, i.e., with increasing temperature of the synthesis.

Figure 2a shows typical isotherms of nitrogen adsorption on the calcined SiO_2–MMS samples examined. Based on these isotherms, we plotted comparative graphs, which are shown in Fig. 2b. The main texture parameters of the SiO_2–MMS were calculated from these graphs by the method described in [27] (Table 2).

It follows from Table 2 that the samples can be divided into three subgroups according to the numerical values of texture parameters and to the character of changes in these parameters with the time of hydrothermal treatment. The first subgroup includes only sample C16-0 (the primary mesophase). The second subgroup consists of samples C16-3, C16-7, C16-20, and C16-63, in which the mesopore volume (V_M), diameter (d_ε), and surface area (A_M) monotonically increased, and the average wall thickness (h_w) monotonically decreased as the duration of hydrothermal treatment increased from 3 to 63 h. The third subgroup is composed of samples C16-63, C16-188, and C16-404, in which all the analyzed texture parameters remained virtually constant as

Table 1. X-ray diffraction and chemical characteristics of SiO_2–MMS samples

Sample	Synthesis temperature, °C	Initial sample			Calcined sample			
		d_{100}, nm	a_0, nm	NR_4/SiO_2 (mol/mol)	d_{100}, nm	a_0, nm	$B[d_{100}]$	D, nm
C16-0	20	3.847	4.442	0.249	3.240	3.741	0.41	28
C16-3	120	4.187	4.835	0.209	3.946	4.556	0.23	67
C16-7	120	4.187	4.835	0.201	3.946	4.556	0.26	57
C16-20	120	4.187	4.835	0.204	3.946	4.556	0.24	62
C16-63	120	4.187	4.835	0.197	3.946	4.556	0.22	76
C16-188	120	4.216	4.868	0.198	3.946	4.556	0.22	76
C16-404	120	4.216	4.868	0.193	3.997	4.615	0.22	76

the duration of the hydrothermal treatment increased from 63 to 404 h.

On going from the first to the second and then to the third subgroup, only the V_M and d_ε values progressively increased. The changes of the specific surface area of mesopores A_M and of the average wall thickness h_w in this sequence are of a more complex (nonmonotonic) character.

In all cases, the external surface area of blocks A_{ext} (the external surface area of mesophase particles) tends to decrease with the increasing duration of the hydrothermal treatment.

DISCUSSION

1. Cold Mixing Step

As follows from published data (see, for example, [17, 24]) and the above experimental results, the formation of the SiO_2–MMS silicate mesophases from soluble silicates and Cn-alkyltrimethylammonium salts via the S^+I^- reaction path proceeds even at room temperature at the stage of simple mixing of aqueous solutions of the specified compounds prior to treatment of the reaction mixtures under hydrothermal conditions. Contrary to the recently published viewpoint [1], these systems like C16-0 are thermally stable. Indeed, after oxidative heat treatment at 550–580°C, which resulted in the removal of surfactant cations, they not only retained a significant volume of mesopores (Table 2) but also were characterized by the presence of X-ray reflections, including not only (100) reflections but also reflections of a higher order (Fig. 1, curve *1*). These facts are consistent with the data published previously [17]. Thus, even at the stage of synthesis ($t = 0$), the system should be considered as the primary mesophase with a hexagonal packing of cylindrical mesopores 3.13 nm in diameter (Table 2). As was found in special measurements by small-angle X-ray scattering, only separate cylindrical micelles with the average diameter $d_{mcl} \cong$ 3.6 nm are present in an aqueous surfactant solution with the molar ratio $H_2O/C_{16}H_{33}N(CH_3)_3Br \cong 340$ at

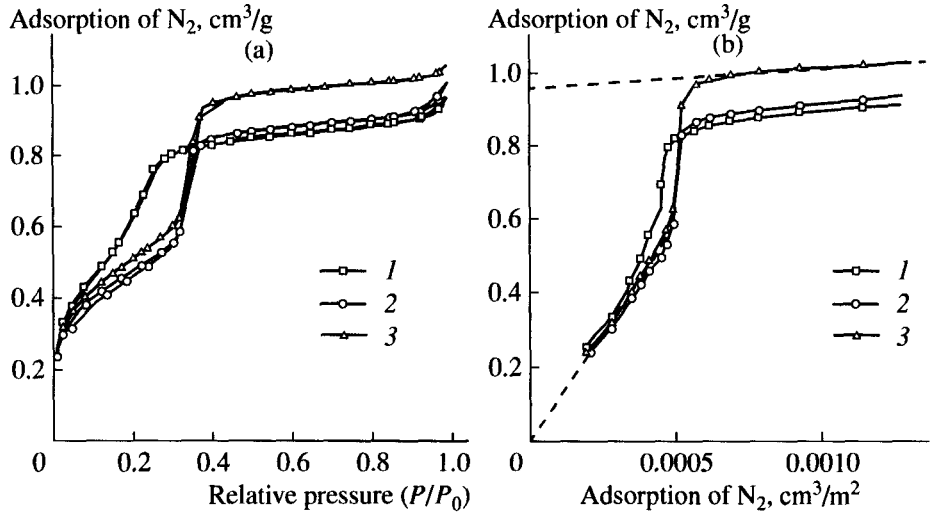

Fig. 2. (a) Nitrogen adsorption isotherms for calcined SiO_2–MMS samples of the C16 series and (b) comparative graphs plotted on the basis of these isotherms. The duration of hydrothermal treatment, h: (*1*) 0, (*2*) 3, and (*3*) 404.

Table 2. Texture parameters of calcined SiO_2–MMS samples

Sample	Specific surface area, m^2/g		V_M, cm^3/g	d_e, nm	h_w, nm
	A_M	A_{ext}			
C16-0	1173	82	0.810	3.13	0.62
C16-3	993	90	0.824	3.81	0.74
C16-7	984	99	0.850	3.84	0.72
C16-20	1083	84	0.885	3.87	0.69
C16-63	1107	64	0.942	3.90	0.65
C16-188	1105	36	0.939	3.90	0.65
C16-404	1114	57	0.951	3.96	0.65

20°C. Any aggregates or products of a larger size are almost absent. Thus, it is believed that it is these micelles that react with silicate ions by the S^+I^- mechanism upon mixing corresponding solutions.

At the same time, spontaneous precipitation of the hexagonal mesophase (any of the silicate anions present in solution can participate in this mesophase) must be necessarily accompanied by the formation of fine particles having a significantly disordered (defect) structure. Indeed, of all the samples examined (see Table 1), C16-0 is characterized by the smallest linear dimension of the coherent scattering region. The degree of volume shrinkage of the structure on going from the initial to the calcined form, which is determined by the equation [28]

$$(1 - f_v) = [1 - (V_{calc}/V_{init})] \cong [1 - (d_{100}^{calc}/d_{100}^{init})^2],$$

is maximum (~30%) for this sample.

2. *Thermal Treatment Step*

The hydrothermal treatment of the primary mesophase in a mother liquor at 120°C for 3 h or longer resulted in detectable changes of many properties of SiO_2–MMS.

First, the a_0 parameter of the hexagonal lattice abruptly increased (cf. samples C16-0 and C16-3, Table 1). Next, at $t \geq 3$ h, this parameter remained almost unchanged. This dramatic change in the a_0 parameter after the onset of hydrothermal treatment of the reaction mixture was observed previously [14]. It was explained by the phase transformation of the primary mesophase with a layered structure into a mesophase with the hexagonal type of packing. This explanation seems to be incorrect because the primary mesophase is just a mesophase with the hexagonal structure (Fig. 1, curve *1*).

At the same time, the conditions of synthesis of C16-0 and C16-3 mesophases differ in the composition of the starting mixtures and in the duration of the treatment only slightly. However, they considerably differ in temperature (20 and 120°C, respectively). It is likely that this factor is primarily responsible for the abrupt increase in the unit cell parameter a_0. Indeed, it is well known [29] that the internal structure of a cylindrical surfactant micelle is formed by hydrophobic C_{16}-hydrocarbon tails, which are directed inside the micelle and form the micellar volume. Hydrophilic ammonium heads are located at the interface between this volume and the phase of an aqueous solution and form a positively charged surface of the micelle. The volume, and hence the diameter, of the micelle is proportional to the kinetic volume occupied by each of the tails. An increase in the temperature of such a micellar solution must be necessarily accompanied by an increase in the kinetic volume occupied by each of the tails and hence by an increase in the volume and diameter of the micelle itself. It is likely that an initial silicate ion coating, which is spontaneously formed around micelles at the step of coprecipitation, hardly represents a barrier to this "thermal" expansion. Note that, to a first approximation, this "thermal" expansion of a micelle is analogous to a well-known increase (or decrease) in the micellar volume (and diameter) as a result of an increase (or decrease) in the length of the tail in Cn-alkyltrimethylammonium compounds under isothermal conditions.

Second, the chemical composition of the initial forms of SiO_2–MMS changed upon heating (Table 1): the concentration of alkyltrimethylammonium cations decreased. A pronounced (practically abrupt) change occurred during the first several hours of hydrothermal treatment. Two reasons can be responsible for the change in the mesophase composition with increasing temperature. On the one hand, although the interaction of cationic surfactant micelles and anionic SiO_2 species proceeds to a large extent even at room temperature on mixing solutions, additional incorporation of free silicate anions from the mother liquor into the structure of the silicate coatings of micelles can further occur under hydrothermal conditions at an elevated temperature. The above "thermal" expansion of silylated micelles in the composition of the primary mesophase, which is accompanied by healing the defects in the structure of the silicate coating, can be responsible for this incorporation. On the other hand, an increase in the treatment temperature can result in an increase in the degree of hydrolysis in the surfactant cation–silicate anion system with the formation of alkyltrimethylammonium hydroxide followed by its transfer to the mother liquor from the composition of the mesophase. However, the available experimental data cannot give preference to any of the above reasons. This important problem will be the subject for future studies.

With increasing duration of hydrothermal treatment, there are two tendencies: on the one hand, an increase in the linear dimension of the coherent scattering region (the D value in Table 1) and, on the other hand, a decrease in the external surface area of particles that form the mesophase (the A_{ext} value in Table 2). These changes suggest that the average size of ordered ele-

mentary blocks (particles) of SiO_2–MMS increases in the course of hydrothermal treatment.

3. Change in Texture Parameters

The adsorption method [27] provides an opportunity to calculate the texture parameters of SiO_2–MMS only after thermal treatment and evacuation, which result in the removal of an organic component and in dehydration of the sample. The removal of the surfactant from the mesophase during the oxidative heat treatment serves to empty the micellar pores of the organic substance present in them and to form a material with a hexagonal packing of cylindrical mesopores of a particular size. In calcined SiO_2–MMS samples, these mesopores are separated from each other by a wall of silicon dioxide, which has a thickness (h_w) of 0.62–0.74 nm in all the samples examined (Table 2). This dimension approximately corresponds to the size of two silicon–oxygen tetrahedra with a common oxygen atom. At the same time, as can be seen in Table 2, the wall thickness and the mesopore diameter depend on both the conditions of hydrothermal treatment of the mesophase in a mother liquor (i.e., on the synthesis temperature) and on the duration of this treatment (i.e., on the time of hydrothermal synthesis).

As the temperature of the synthesis increases, the thermal expansion of micelles and the possible incorporation of additional silicate anions into the mesophase result in an abrupt increase (Table 2, samples C16-0 and C16-3) in both the mesopore diameter d_ε and the average wall thickness h_w. As was found previously [27], a regular decrease in the specific surface area of mesopores A_M is a direct consequence of increasing h_w.

An increase in the duration of hydrothermal treatment at a constant temperature to 63 h results in a further (however, monotonic) increase in d_ε and in a decrease in h_w. Assuming that the internal structure of a surfactant micelle is independent of the residence time under these isothermal conditions, we can conclude that monotonic changes in d_ε and h_w must be precisely associated with changes in the wall structure.

Indeed, the defect structure of walls in a spontaneously formed primary mesophase of the C16-0 type results from the following processes: (1) condensation of SiOH groups, which requires a certain mutual orientation of these groups, between neighboring silicon–oxygen tetrahedra is obviously not completed; (2) water molecules can be located between some tetrahedra in the structure of the silicate wall; (3) the surface of micelles can be coated with silicate anions of different types, and the coverage can be incomplete. It is likely that a long hydrothermal treatment will facilitate an optimum mutual orientation of silicon–oxygen tetrahedra, which results in an increase in the degree of polycondensation of neighboring SiOH groups. A monotonic decrease in the wall thickness and a simultaneous increase in the apparent diameter of mesopores in calcined samples (Table 2) are the consequences of these rather slow transformations.

A further increase in the duration of hydrothermal treatment at a constant temperature (over 63 h) does not cause any considerable changes in either the structure (Table 1) or the texture parameters of SiO_2–MMS. This fact, on the one hand, provides an indirect support for the above assumption on the slow ordering of the wall structure and, on the other, suggests that a rather stable steady state exists in the SiO_2–MMS under the examined conditions. The latter circumstance unambiguously demonstrates that, in the course of synthesis under hydrothermal conditions at 120°C with duration up to 400 h, the SiO_2–MMS undergoes no irreversible transformations other than those described above.

4. Mechanism of the Process

Thus, to a first approximation, the formation of the SiO_2–MMS under hydrothermal conditions is similar to the crystallization of SiO_2 from solutions. It involves both the transfer of the silicate material from the solution to the solid phase and an increase in the size of the ordered particles of this phase. The principal difference is as follows: cylindrical cationic surfactant micelles act as an organizing agent in the formation of SiO_2–MMS.

Figure 3 schematically represents the mechanism described. In this regard, it is in complete agreement with the concept of a macromechanism of formation of SiO_2–MMS at a micellar level. This mechanism was developed previously [12, 13] and discussed repeatedly in recent literature [1–3]. On mixing a silicate solution with a cationic surfactant solution, in which individual cylindrical micelles are already formed, the rapid anion–cation interaction S^+I^- occurs at the surface of micelles. In the examined pH region (10.5–11.5), SiO_2 forms a number of soluble species. It is suggested [14, 18] that these species equally participate in the multicenter (polydentate) interaction with the charged surface of micelles. However, the polydentate coverage with silicate oligomers will necessarily complicate the formation of both a reasonably uniform thin silicate layer and an ordered mesophase in general. Only micelles covered with silicate anions that are optimum with respect to the charge and morphology will participate in the formation of a highly organized material in the course of self-assembling at near-room temperatures. Conceivably, these micelles are single-charged monomers. If silylated micelles with nonoptimal characteristics are involved in the self-assembling process, the degree of organization of the obtained mesophase material will necessarily decrease. This decrease can manifest itself, for example, in a considerable increase in the half width of reflections in the X-ray diffraction pattern.

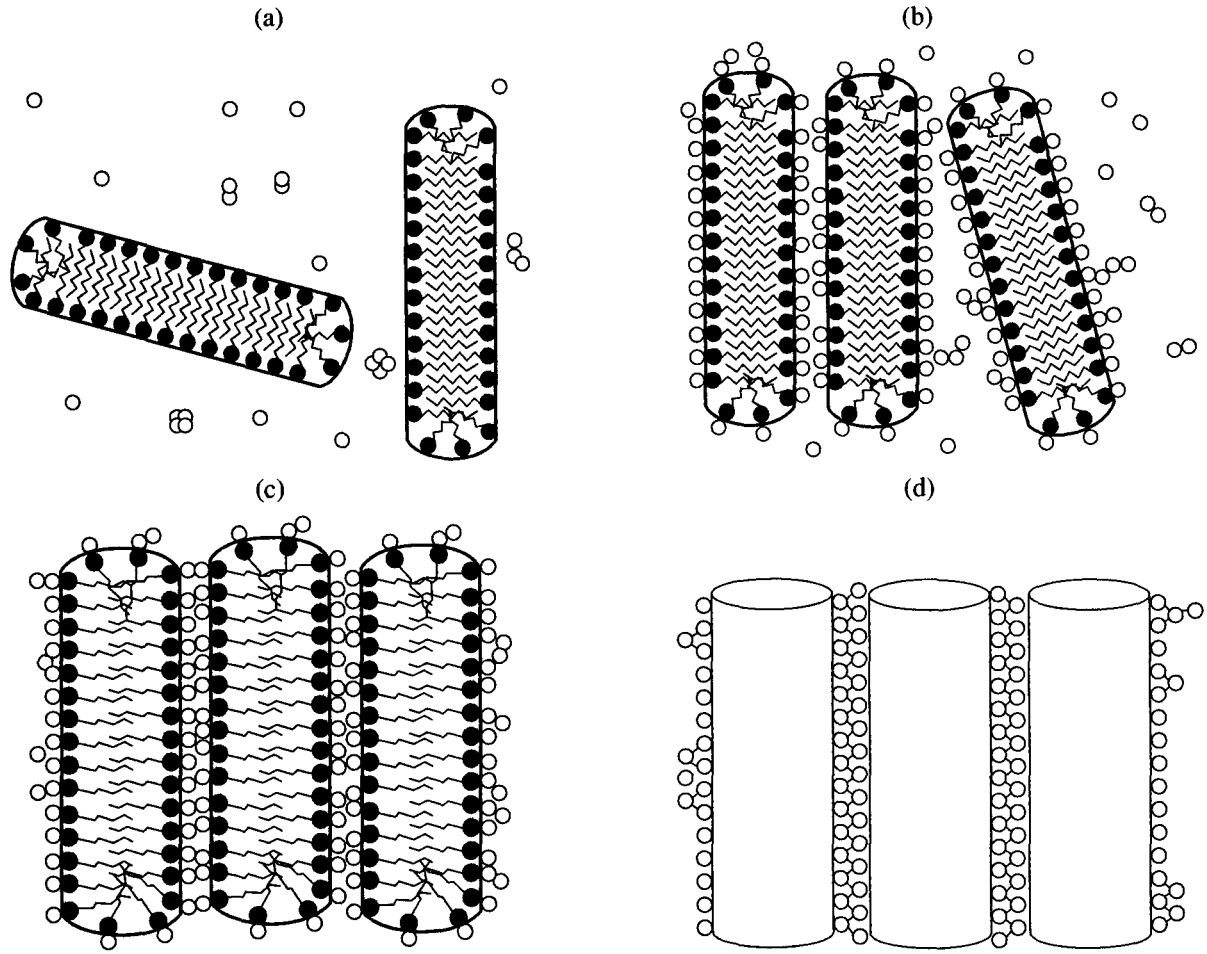

Fig. 3. Schematic diagram of the mechanism of formation of SiO_2–MMS with the participation of cationic surfactants. Processes involving only the key ions are presented: (a) initial ions in an aqueous solution are cationic surfactant micelles and silicate anions; (b) silylated micelles; the onset of low-temperature self-assembling; (c) hydrothermal treatment; an increase in the micelle diameter; ordering and polycondensation in the silicate wall; and (d) a silicate mesophase after oxidative heat treatment. Notation: closed circles are cetyltrimethylammonium cations, and open circles are silicate tetrahedra.

The mechanism of self-assembling of optimally silylated micelles is not considered in this work. We assume that, as a first approximation, it is identical to general self-assembling mechanisms for micellar systems [29, 30]. This mechanism is also supported by the fact that the lattice parameter a_0 for the initial form of the primary SiO_2–MMS (sample C16-0) depends on only the micelle diameter. Indeed, the a_0 parameter for sample C16-0 is 4.44 nm (Table 1). As mentioned above, the diameter of C_{16} micelles (d_{mcl}) in an aqueous $C_{16}H_{33}N(CH_3)_3Br$ solution with the molar ratio $H_2O/NR_4Br \cong 340$ at 20°C is equal to 3.6 nm. Consequently, the wall thickness in sample C16-0 is $h_w^{init} = a_0 - d_{mcl}^{20°C} = 4.44 - 3.6 \cong 0.84$ nm. This is consistent with the concept of the formation of the wall with a thickness of two tetrahedra in the completely hydrated (loosened) state. It is likely that this primary C_{16} mesophase, which is rapidly formed even at room temperature, is rather stable in time [17] if it is not subjected to any external action such as heating.

Changes in d_ε and h_w and related changes in V_M and A_M were observed upon hydrothermal treatment. In general, these changes are the consequences of the micromechanism (at a molecular level) of building the silicate walls in SiO_2–MMS.

As mentioned above, rapid spontaneous self-assembling, which occurs even at room temperature, necessarily results in the formation of a defect structure. As a particular result, the silicate wall thickness at this step of the synthesis ($h_w^{init} \cong 0.84$ nm) is much greater than the wall thickness h_w (Table 2) after oxidative heat treatment, which is accompanied by the complete polycondensation of neighboring OH groups.

Hydrothermal treatment dramatically affects the state of the system under consideration: the micelle diameter increases; new silicate anions are involved in the wall formation; the silicate coating of micelles containing anions coordinated by the polydentate mechanism is optimized, and these micelles are involved in the building and enlargement of mesophase blocks; and the probability of the optimum orientation of neighbor-

ing silicon–oxygen tetrahedra increases to facilitate more complete polycondensation in the wall. The formation of siloxane bonds (Si–O–Si) results in an increase in the packing density of these tetrahedra, in exclusion of water molecules, and, ultimately, in a maximum decrease in h_w.

Generally, all physicochemical processes that are responsible for the formation of SiO_2–MMS are continuous functions of the temperature and duration of the synthesis, of the composition of the initial reaction mixture, and of some other parameters that specify external conditions for these processes. Thus, both the primary defect structure of a mesophase spontaneously precipitated at near-room temperatures [17] and the ordered structure of SiO_2–MMS formed under conditions of hydrothermal treatment at 120°C (Tables 1, 2) should be considered as different quasi-steady states of the SiO_2–MMS system. In all cases, a quasi-steady state is taken to mean that the rate of attaining such a state is much higher than the rate of its decay under unchanged external conditions. In particular, at 120°C under batch conditions, a quasi-steady state of the system was attained after approximately 60 h and then remained almost unchanged at least for 300 h (Tables 1, 2).

Variations in the external conditions of formation of SiO_2–MMS should be expected to necessarily result in changes in not only the structure of the quasi-steady-state system but also the time of its reasonably stable existence.

In summary, the results of this study demonstrate that the principal mechanism of formation of SiO_2–MMS discussed in the literature (liquid crystal templating) corresponds to only the macroscopic level of description; this mechanism occurs on the background of subtle microscopic molecular mechanisms. These latter describe the effect of hydrothermal treatment on the structure and texture characteristics of samples, the degree of shrinkage, etc. These mechanisms can be the subject of future studies of the state of inorganic dopants, mechanisms of the growth of mesophase blocks, factors controlling the thermal stability of the system, etc.

ACKNOWLEDGMENTS

This work was supported by the Russian Foundation for Basic Research (project no. 98-03-32390a).

REFERENCES

1. Corma, A., *Chem. Rev.*, 1997, vol. 97, no. 6, p. 2373.
2. Raman, N.K., Anderson, M.T., and Brinker, C.J., *Chem. Mater.*, 1996, vol. 8, p. 1682.
3. Sayari, A., *Chem. Mater.*, 1996, vol. 8, p. 1840.
4. Corma, A., *Top. Catal.*, 1997, vol. 4, p. 249.
5. Sayari, A. and Liu, P., *Microporous Mater.*, 1997, vol. 12, p. 149.
6. Huang, Y.-Y., McCarthy, T.J., and Sachtler, W.M.H., *Appl. Catal., A*, 1996, vol. 148, p. 135.
7. Antonelly, D.M. and Ying, J.Y., *Angew. Chem., Int. Ed. Engl.*, 1995, vol. 34, p. 2014.
8. Antonelly, D.M. and Ying, J.Y., *Chem. Mater.*, 1996, vol. 8, p. 874.
9. Antonelly, D.M. and Ying, J.Y., *Angew. Chem., Int. Ed. Engl.*, 1996, vol. 35, p. 426.
10. Antonelly, D.M., Nakahira, A., and Ying, J.Y., *Inorg. Chem.*, 1996, vol. 35, p. 3126.
11. Sun, T. and Ying, J.Y., *Nature*, 1997, vol. 389, p. 704.
12. Kresge, C.T., Leonowicz, M.E., Roth, W.J., *et al.*, *Nature*, 1992, vol. 359, p. 710.
13. Beck, J.S., Vartuli, J.C., Roth, W.J., *et al.*, *J. Am. Chem. Soc.*, 1992, vol. 114, p. 10834.
14. Monnier, A., Schuth, F., Huo, Q., *et al.*, *Science*, 1993, no. 261, p. 1299.
15. Huo, Q., Margolese, D.I., Ciesla, U., *et al.*, *Nature*, 1994, vol. 368, p. 317.
16. Beck, J.S., Vartuli, J.C., Kennedy, G.J., *et al.*, *Chem. Mater.*, 1994, vol. 6, p. 1816.
17. Cheng, C.-F., Luan, Z., and Klinowski, J., *Langmuir*, 1995, vol. 11, p. 2815.
18. Firouzi, A., Kumar, D., Bull, L.M., *et al.*, *Science*, 1995, vol. 267, p. 1138.
19. Kushalani, D., Kuperman, A., Ozin, G.A., *et al.*, *Adv. Mater.*, 1995, vol. 7, p. 842.
20. Inagaki, S., Sakamoto, Y., Fukushima, Y., *et al.*, *Chem. Mater.*, 1996, vol. 8, p. 2089.
21. Corma, A., Kan, Q., Navarro, M.T., *et al.*, *Chem. Mater.*, 1997, vol. 9, p. 2123.
22. Sayari, A., Liu, P., Kruk, M., *et al.*, *Chem. Mater.*, 1997, vol. 9, p. 2499.
23. Kruk, M., Jaroniec, M., Ryoo, R., *et al.*, *Microporous Mater.*, 1997, vol. 12, p. 93.
24. Lin, H.-P., Cheng, S., and Mou, C.-Y., *Microporous Mater.*, 1997, vol. 10, p. 111.
25. Yoegtlin, A.C., Matijasic, A., Patarin, J., *et al.*, *Microporous Mater.*, 1997, vol. 10, p. 137.
26. Karnaukhov, A.P., Fenelonov, V.B., and Gavrilov, V.Yu., *Pure Appl. Chem.*, 1989, vol. 61, p. 1913.
27. Fenelonov, V.B., Romannikov, V.N., and Derevyankin, A.Yu., *Micropor. Mesopor. Mater.*, 1999, vol. 28, p. 57.
28. Romannikov, V.N., Fenelonov, V.B., Paukshtis, E.A., *et al.*, *Micropor. Mesopor. Mater.*, 1998, vol. 21, p. 411.
29. Gelbert, W.M. and Ben-Shaul, A., *J. Phys. Chem.*, 1996, vol. 100, p. 13169.
30. Hyde, S.T., *Colloque De Physique*, 1990, vol. 57, p. 7.